

# Theory of Modulated Phases in Tethered Polymer Monolayers

N. A. Spenley<sup>†</sup>

Max-Planck-Institut für Kolloid- und Grenzflächenforschung, Kantstr. 55, 14513 Teltow, Germany

Received September 30, 1996; Revised Manuscript Received February 23, 1998

**ABSTRACT:** The phase behavior of tethered polymer monolayers is studied theoretically. These layers are formed at the air–water interface by hydrophobic polymers with a hydrophilic endgroup, the effect of the endgroup being to anchor the end of the polymer at the interface, forming a brush. A mixed layer of two incompatible polymers should exhibit modulated phases, arising from the competition between demixing and electrostatic forces. The phase behavior is calculated in terms of the density of polymer and the degree of polymerization. Stripe phases are found to occur for sufficiently high molecular weight.

## 1. Introduction

Many different physical systems exhibit so-called “modulated phases”, in which an order parameter varies periodically in space. In general, they arise from the competition between a long-range attractive force and a short-range repulsive force. For example, the lamellar and other phases in block copolymer melts are due to the demixing effect, which tends to segregate the two monomer types (repulsive), and the chemical connectivity of the polymers, which keeps them together (attractive). A review is given by Seul and Andelman.<sup>1</sup> This paper is devoted to the theory of such phases in polymer monolayers.

A suitable layer may be created using an insoluble macromolecule with a hydrophilic headgroup. If such molecules are spread onto the water surface, the headgroup enters the water while the remainder of the molecule remains above the surface. If the surface density of molecules is high enough, then they form a continuous film. The hydrophilic group tethers the polymer to the interface, while the rest of the molecule is stretched upward to form a brush. Such layers (consisting of one component) have been prepared, using perfluoropolyethers<sup>2</sup> and polyisoprenes<sup>3</sup> and appear to be reasonably well described by the self-consistent field theory of polymer brushes.<sup>4,5</sup> A layer composed of two different polymers would tend to separate, like a bulk mixture.<sup>6</sup> However, if the two species have oppositely charged headgroups, there will be the competition of interactions associated with modulated phases. The order parameter is then the composition, and the short-range interaction is the van der Waals and other forces leading to chemical incompatibility and demixing of the two species. The long-range interaction is the Coulomb force. Modulated phases have already been observed in Langmuir monolayers of small amphiphiles<sup>1,7,8</sup> and studied theoretically<sup>9,10</sup> (in fact, they are seen with a single component, because of the complicated phase behavior of these layers). Attempts to create a mixed layer of two polymers are now in progress,<sup>11</sup> so it seems opportune to develop a theory of modulated phases in polymer monolayers. In this paper, the polymer character of the problem is emphasized. The molecular weight of a polymer may be varied over a large range.

This can be used as a tuning parameter to control the strength of the interaction, and the effect of this on the monolayer is calculated. The strength of the polymer–polymer interaction is described by a  $\chi$ -parameter, as is usual in theoretical studies of polymers, and the numerical calculations and estimates are made using values appropriate for a polymeric monolayer. Phenomenological or fitting parameters are avoided, so direct predictions can be made.

We introduce the following definitions. Let  $\sigma$  be the number of polymers per unit area (the “grafting density”), and  $N$  be the degree of polymerization of the polymer. The thickness of the layer is  $L$ . No solvent is present, so  $L = N\nu\sigma$  where  $\nu$  is the volume per monomer. The step length is denoted by  $b$ , so the end-to-end length of the polymer is  $L_0 = bN^{1/2}$ . Temperatures will be represented by  $T$  and measured in units of  $k_B$  (i.e.  $k_B$  is defined to be 1). The headgroup carries a charge  $pe$  ( $e$  being the elementary charge). For a pure layer (i.e., with one component) the main contributions to the free energy come from the electrostatic interaction between the headgroups,  $F_{es}$ , from the stretching energy of the polymers,  $F_{stretch}$ , from the contact energies (surface tensions) between the air, water, and polymer,  $F_{ST}$ , and from the configurational entropy of the molecules,  $F_{conf}$ .

$$F = F_{es} + F_{stretch} + F_{ST} + F_{conf} \quad (1)$$

We take these quantities to be per unit area. The usual self-consistent theory for a dry (solvent-free) brush may be applied, so  $F_{stretch} = (\pi^2/8)\sigma^3 N\nu^2/b^2$ . The electrostatic energy  $F_{es}$  is calculated in section 2. The configurational term is  $F_{conf} = T\sigma(\ln \sigma - 1)$ . The remaining contribution,  $F_{ST}$ , is just a constant,  $\gamma$ , which is calculated relative to the surface energy of the air–water interface

$$F_{ST} = \gamma = \gamma_{ap} + \gamma_{wp} - \gamma_{aw} \quad (2)$$

where  $\gamma_{ap}$ ,  $\gamma_{wp}$  and  $\gamma_{aw}$  are the surface energies for the air–polymer, water–polymer, and air–water interfaces respectively.

We may suppose a mixed monolayer to be composed of polymers of two different chemical species, A and B, in proportions  $\phi$  and  $1 - \phi$  respectively. The headgroup charges are  $p_A$  and  $p_B$  respectively. If the two species

<sup>†</sup> Present address: Unilever Research, Port Sunlight Laboratory, Quarry Road East, Bebington, Wirral L63 3JW, U.K.

mix, the free energy has entropic and mixing energy terms

$$F = F_{\text{es}}(\phi) + F_{\text{stretch}} + F_{\text{ST}} + \sigma TN\chi\phi(1 - \phi) + \sigma T(\phi \ln \sigma\phi + (1 - \phi) \ln \sigma(1 - \phi)) \quad (3)$$

where these have been calculated at the level of Flory–Huggins theory. We assume that the stretch energy  $F_{\text{stretch}}$  and surface tension  $F_{\text{ST}}$  are unchanged from the pure monolayer. This should be valid as long as  $\gamma$  is not too different for the two species, and we restrict ourselves to the case where  $L_0$  for A is equal to  $L_0$  for B. If the two species have the same charge, then the electrostatic energy is also unchanged. Depending on  $N$  and  $\chi$ , they will either mix or undergo macroscopic phase separation (in two dimensions).<sup>12,13</sup> At the level of the present theory, the phase diagram will be identical to that for polymers in the bulk.

If the two molecules have opposite charges, then, in the mixed state, these will tend to cancel, reducing the electrostatic energy. The long-range electrostatic interaction will then tend to favor mixing, while the short-range  $\chi$  term favors demixing. The result may be some kind of modulated phase. The free energy of such a phase is no longer given by eq 3 but will be derived later. We anticipate that the allowed phases will be composed of alternating stripes of different compositions, or else of circular domains in a hexagonal array. These are the phases observed in other two-dimensional modulated systems.<sup>1</sup> They will be referred to as the stripe (S) and hexagonal (H) phases. The mixed state will be called D (for disordered) and a phase consisting of one component only (i.e.,  $\phi = 0$  or 1) will be P (pure).

In the remainder of this paper, the free energies of the different phases will be calculated and compared. In section 2, the electrical energy of a single-component or uniformly mixed layer is given. In section 3, the stability of the layer is considered. Section 4 discusses the electrical energy of a modulated phase, and section 5, the other contributions. Section 6 describes the resulting phase diagram, and section 7 is the conclusion.

## 2. Electrostatic Energy of a Pure Monolayer

In this section, we will calculate the contribution to the free energy from the electrostatic interaction between the headgroups, using the usual Gouy–Chapman theory of the electrical double layer.<sup>14,15</sup> Each polymer in the monolayer has a headgroup which dissociates in the water. We will model the charged polymer headgroups as a continuous layer at the polymer/water interface

$$\rho(\mathbf{r}) = \rho_0 \delta(z) \quad (4)$$

where  $\rho_0$  is the average charge per unit area. For a single-component layer,  $\rho_0 = pe\sigma$ . Here, the polymer–water interface is at  $z = 0$ , and the space  $z > 0$  is occupied by water. The distribution of ions is then given by a Poisson–Boltzmann equation

$$\nabla^2 \psi + \frac{2n_0 e}{\epsilon} \sinh(e\psi/T) = -\frac{\rho}{\epsilon} \quad (5)$$

where  $\psi$  is the potential,  $n_0$  is the bulk density of ions,  $e$  is the unit charge and  $\epsilon$  is the permittivity of water. Note that it is necessary to allow for ions of both positive

and negative charge, since both of these are present in water. To include only the counterions (by having exp instead of sinh in eq 5) leads to an inconsistent approximation (a divergent result is obtained for the potential). The potential at the headgroup layer is<sup>14</sup>

$$\psi(0) = 2 \sinh^{-1}(\rho_0/4e\sigma_0) \quad (6)$$

where  $\sigma_0 = \epsilon T\kappa/2e^2$  and  $\kappa^{-1} = (\epsilon T/2n_0e^2)^{1/2}$  is the Debye length. (We are assuming that the permittivity of polymer is much less than that of water, which is realistic.) The electrostatic energy of the headgroup charges, per unit area, is

$$E_0 = \int_0^{\rho_0} \psi(0) d\rho_0 = \frac{2T\rho_0}{e} \left( \sinh^{-1} \tilde{\rho} + \frac{1 - (1 + \tilde{\rho}^2)^{1/2}}{\tilde{\rho}} \right), \quad \tilde{\rho} = \frac{\rho_0}{4e\sigma_0} \quad (7)$$

The usual result for the free energy of an electrical double layer also includes a contribution associated with the adsorption or dissociation process which creates the layer.<sup>14</sup> For the present purpose, this contribution may be left out, as long as the monolayer is assumed to be fully dissociated.

For  $\rho_0 \ll e\sigma_0$ , we have the weak-charge limit

$$E_0 = \rho_0^2/2\epsilon\kappa \quad (8)$$

and for  $\rho_0 \gg e\sigma_0$ , we have the strong-charge limit

$$E_0 = (2T\rho_0/e)(\ln(\rho_0/2e\sigma_0) - 1) \quad (9)$$

For water at room temperature without added salt,  $\kappa^{-1} \approx 1.0 \mu\text{m}$  and  $\sigma_0 = 5.8 \times 10^{-7} \text{Å}^{-2}$ . For the polymer monolayer, the charge density is on the order of one elementary charge per 100 Å<sup>2</sup>. This gives  $\rho_0/e\sigma_0 \approx 17\,000$ , so we are well into the strong-charge regime. From now on, we will use only the limiting case, eq 9.

## 3. Surface Pressure and Stability of the Layer

The surface pressure of the monolayer may be measured experimentally in a Langmuir trough. If  $F$  is the free energy of the system per unit area,  $N_P$  is the total number of polymers, and  $A$  is the total area, then the surface pressure is given by

$$\gamma_{\text{SP}} = -\left(\frac{\partial FA}{\partial A}\right)_{N_P} \quad (10)$$

Notice that the total number of polymers,  $N_P$ , is held constant. The free energy is as given in eq 1, and the electrostatic energy is  $E_0$ , as calculated in the previous section. The result is

$$\gamma_{\text{SP}} = (1 + 2p)\sigma T + \frac{\pi^2}{4} \frac{Nv^2 T}{b^2} \sigma^3 - \gamma \quad (11)$$

The first term comes from the electrostatic energy and from the configurational entropy, the second comes from the stretching energy of the polymers, and the third is the contact energy. In general, the stretching term will dominate. An earlier estimate of  $\gamma_{\text{SP}}$  was made by Goedel *et al.*<sup>2</sup> Their expression was similar, but the first term was only  $2\sigma T$ , for  $p = 1$ . This is because they

neglected the electrostatic interaction and treated the counterion cloud as an ideal gas in two dimensions. The present calculation takes into account both the entropic (i.e. ideal gas) and energetic contributions to the free energy.

At low densities of polymer, the film will not be continuous but will be ruptured by surface tension. The accessible range of  $\sigma$  is therefore bounded below by some value  $\sigma_{\min}$ . It is also bounded above because the density cannot exceed one polymer per monomer cross-sectional area.

It is possible to calculate  $\sigma_{\min}$  by examining the surface pressure, because the film will rupture just when the pressure becomes negative. Setting  $\gamma_{\text{SP}}$  to zero gives

$$\sigma_{\min}^3 = \frac{4}{\pi^3} \frac{b^2 \gamma}{TNv^2} \quad (12)$$

neglecting the first term in  $\gamma_{\text{SP}}$  as an approximation. For polyisoprene,  $b = 6 \text{ \AA}$ ,  $v = 124 \text{ \AA}^3$ , and  $\gamma = 13 \times 10^{-3} \text{ N m}^{-1}$ .<sup>3</sup> This gives

$$\sigma_{\min} = 0.031 N^{-1/3} \text{ \AA}^{-2} \quad (13)$$

This expression gives reasonable agreement with the experimental data of ref 3. It will be useful later in determining the accessible part of the phase diagram.

#### 4. Electrostatic Energy of a Modulated Phase

We will consider here the two different modulated phases, hexagonal and striped. Assuming that each domain type is composed of either pure A or pure B, then the surface charge density is now  $p_A e \sigma$  inside A domains and  $p_B e \sigma$  inside B domains. To calculate the electrostatic energy in principle requires the Poisson–Boltzmann equation to be solved in three dimensions, which cannot be done analytically. However, if the length scale of the modulation is less than the Debye length, then the modulation is unscreened. The charge distribution may be separated into two parts,  $\rho(\mathbf{r}) = \rho_0 \delta(z) + \rho_{\text{mod}}(x, y) \delta(z)$ , where  $\rho_0$  is the average density, and  $\rho_{\text{mod}}$  is the modulation. The total electrostatic energy is then just  $E_0$ , evaluated for  $\rho_0 = p_A \phi e + p_B(1 - \phi)e$ , plus the contribution from the modulation calculated using ordinary electrostatic theory (without screening).

The modulated phases will be assumed to have perfect order. In practice, there are likely to be some defects, of course, and there is some evidence that true crystalline order is impossible in two dimensions.<sup>16,17</sup> However, well-defined stripe and hexagonal phases have been observed in monolayers and other systems,<sup>1</sup> so this seems a reasonable approximation. The calculation here is quite similar to that of ref 10, except that here Coulomb interactions are considered instead of dipole.

**4.1. Stripe Phase.** In a stripe phase, the charge distribution varies in one direction only, say  $x$ , and takes the form of a rectangular wave. Let  $\lambda$  be the wavelength, then

$$\rho_{\text{mod}} = 2\sigma e \Delta p (1 - \phi), \quad 0 \leq x < \phi \lambda \quad (14)$$

$$= 2\sigma e \Delta p \phi, \quad \phi \lambda \leq x < \lambda \quad (15)$$

where  $\Delta p = (p_A - p_B)/2$ . The wavelength  $\lambda$  is not known *a priori*, but is to be determined by minimizing the free

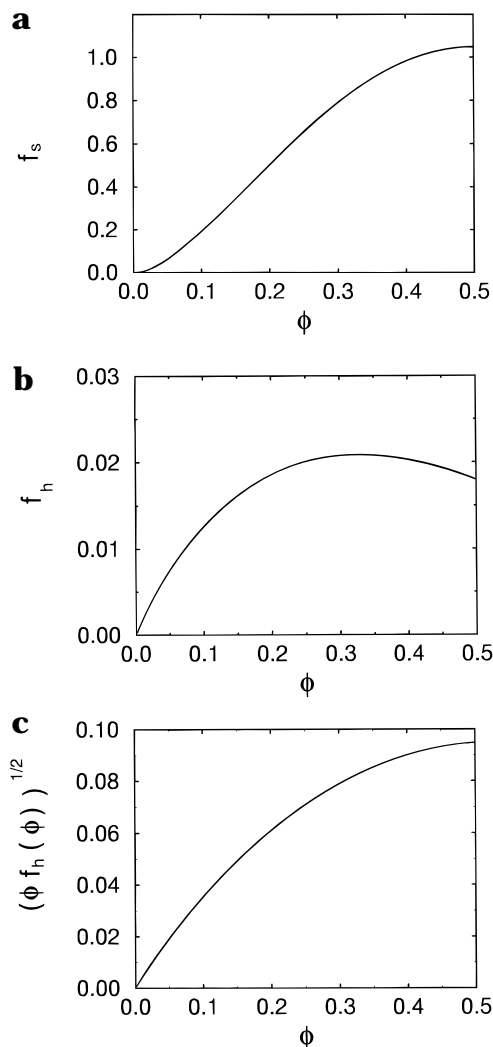


**Figure 1.** The functions (a)  $f_s(\phi)$ , (b)  $f_h(\phi)$  and (c)  $(\phi f_h(\phi))^{1/2}$ .

energy. It may be shown that the energy per unit area of this charge distribution is

$$E_s = \frac{2(\Delta p)^2 \sigma^2 e^2 \lambda}{\pi^3 \epsilon} f_s(\phi) \quad (16)$$

where

$$f_s(\phi) = \sum_{n=1}^{\infty} \frac{\sin^2(n\pi\phi)}{n^3} \quad (17)$$

The function  $f_s$  may be evaluated numerically, and is shown in Figure 1. Note that  $f_s(0.5) = 1.05 \approx 1$ .

**4.2. Hexagonal Phase.** This phase is assumed to consist of a hexagonal array of circular domains. Let  $\lambda$  be the radius of one circle and  $a$  be the lattice constant. If the domains and the matrix are pure A and pure B respectively, then  $\lambda$  and  $a$  are related by

$$(\lambda/a)^2 = 3^{1/2} \phi / 2\pi \quad (18)$$

which is obtained by setting the area of a circle equal to  $\phi$  times the area of a hexagon. The inverse case, with domains of B and a matrix of A, of course corresponds to replacing  $\phi$  by  $1 - \phi$ . The charge densities in the circles and in the matrix are the same as for the stripe phase and are  $2\sigma e \Delta p (1 - \phi)$  and  $2\sigma e \Delta p \phi$  respectively.

The electrostatic energy may be calculated by standard Fourier methods and is found to be

$$E_h = \frac{8(\Delta p)^2 \sigma^2 e^2 \lambda}{\epsilon} f_h(\phi) \quad (19)$$

and

$$f_h(\phi) = \phi^2 \sum_q \frac{J_1(q)^2}{q^3} \quad (20)$$

where  $J_1$  is a Bessel function and the sum is taken over all points on a hexagonal lattice of lattice constant  $3^{-1/4}(8\pi\phi)^{1/2}$ , excepting the origin. The function  $f_h$  must be evaluated numerically, Figure 1.

### 5. Free Energy of Modulated Phases

The free energy of the modulated phases contains a contribution from the interfacial energy between the domains. In the strong segregation limit where the interfaces are narrow compared to the size of one polymer, this may be taken as the total interface area multiplied by a surface tension. We assume that the energy per unit area between polymer domains in the monolayer is the same as that between bulk polymer phases. This was calculated by Helfand and Tagami<sup>18</sup> using self-consistent field theory as

$$\gamma_{AB} = \left(\frac{\chi}{6}\right)^{1/2} \frac{bT}{v} \quad (21)$$

The interdomain area, per unit area of monolayer, is  $2L/\lambda$  for the stripe phase and  $2L\phi/\lambda$  for the hexagonal. Discarding all terms independent of  $\phi$ , we obtain the following expressions for the total free energy of the stripe and hexagonal phases

$$F_s = E_0 + A_s \lambda + B_s / \lambda \quad (22)$$

$$F_h = E_0 + A_h \lambda + B_h / \lambda \quad (23)$$

where

$$E_0 = (2T\rho_0/e) \left( \ln \frac{\rho_0}{2e\sigma_0} - 1 \right) \quad (24)$$

$$\rho_0 = e\sigma(p_A\phi + p_B(1-\phi)) \quad (25)$$

and

$$A_s = \frac{2(\Delta p)^2 \sigma^2 e^2}{\pi^3 \epsilon} f_s(\phi), \quad B_s = \left(\frac{\chi}{6}\right)^{1/2} \frac{2LbT}{v} \quad (26)$$

$$A_h = \frac{8(\Delta p)^2 \sigma^2 e^2}{\epsilon} f_h(\phi), \quad B_h = \left(\frac{\chi}{6}\right)^{1/2} \frac{2LbT\phi}{v} \quad (27)$$

Note that  $E_0$  may be written as

$$E_0 = 4\sigma T \Delta \phi \left( \ln \frac{\sigma \Delta \phi}{\sigma_0} - 1 \right) \quad (28)$$

where  $\Delta\phi$  is defined to be  $(\phi p_A + (1-\phi)p_B)/2$  (this reduces to  $\phi - 1/2$  for  $p_A = -p_B = 1$ ). We can find the

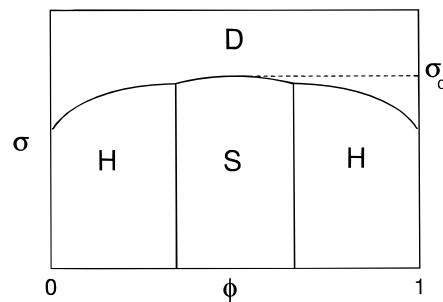


**Figure 2.** The morphology of lowest energy, as a function of surface density  $\sigma$  and composition  $\phi$  (schematic).

preferred size for the microstructure domains by minimizing  $F_s$  and  $F_h$  with respect to  $\lambda$ . The result is

$$\lambda_s = (B_s/A_s)^{1/2} \quad (29)$$

$$\lambda_h = (B_h/A_h)^{1/2} \quad (30)$$

and the free energies are

$$F_s = E_0 + 2(A_s B_s)^{1/2} \quad (31)$$

$$F_h = E_0 + 2(A_h B_h)^{1/2} \quad (32)$$

or explicitly

$$\frac{F_s}{\sigma T} = \frac{E_0}{\sigma T} + \left( \frac{8}{\pi^3} \Delta p f_s(\phi) \left( \frac{\chi}{6} \right)^{1/2} \kappa b N \frac{\sigma}{\sigma_0} \right)^{1/2} \quad (33)$$

$$\frac{F_h}{\sigma T} = \frac{E_0}{\sigma T} + \left( 32 \Delta p \phi f_h(\phi) \left( \frac{\chi}{6} \right)^{1/2} \kappa b N \frac{\sigma}{\sigma_0} \right)^{1/2} \quad (34)$$

The free energy of the disordered phase is

$$\frac{F_d}{\sigma T} = \frac{E_0}{\sigma T} + N \chi \phi (1-\phi) + \phi \ln \phi + (1-\phi) \ln (1-\phi) \quad (35)$$

For a given  $\phi$ , the equilibrium phase is obviously that of lowest free energy. The phase diagram can now be determined in the usual way by minimizing the free energy with respect to the morphology, subject to a fixed overall composition, and allowing for the possibility of phase separation and coexistence. This is done in the next section.

### 6. The Phase Diagram

It is fairly straightforward to determine which morphology has the lowest free energy for given values of  $\phi$  and other parameters. The boundaries between the different regions are found by equating the free energies of the morphologies, and the result is shown schematically in Figure 2. The boundaries between the hexagonal and stripe regions are the lines  $\phi = 0.34$  and  $0.66$ , while the critical point,  $\sigma_c$ , is

$$\frac{\sigma_c}{\sigma_0} = \frac{\pi^3 6^{1/2}}{128} \frac{N \chi^{3/2}}{\Delta p^2 \kappa b} \left( 1 - \frac{4 \ln 2}{N \chi} \right)^2 \quad (36)$$

The true phase diagram will contain some regions of phase coexistence. However, any single-phase regions

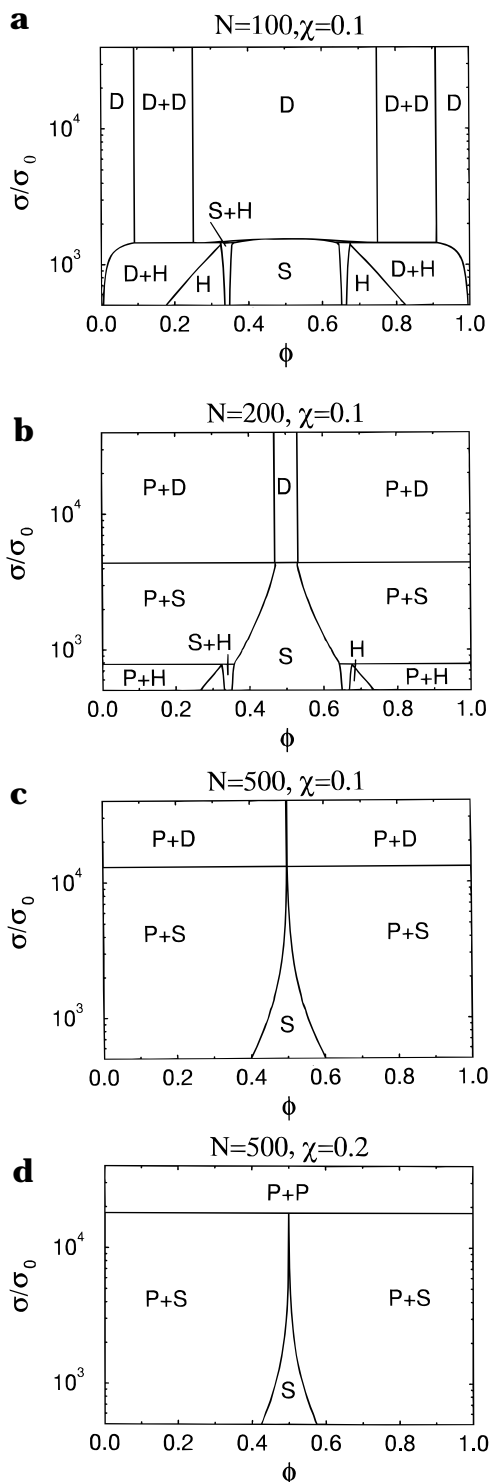


**Figure 3.** Phase diagrams computed for various values of polymerization number  $N$  and Flory parameter  $\chi$ . The vertical axis is the surface density of polymer,  $\sigma$ , in units of  $\sigma_0 = 5.8 \times 10^{-7} \text{ \AA}^{-2}$ , so that  $\sigma/\sigma_0 = 10000$  corresponds to an area per molecule of about  $170 \text{ \AA}^2$ .

must be as in Figure 2. Also, we see that modulated phases (stripe or hexagonal) can occur only for  $\sigma < \sigma_c$ . Figure 3 shows a sequence of phase diagrams for various values of  $N$  and  $\chi$ , calculated using a numerical implementation of the common tangent construction. The diagrams are given naturally in the  $\sigma$ - $\phi$  plane, since  $\sigma$  is the quantity most easily varied in an experiment. The other parameters are all fixed, at reasonable values ( $\kappa = 10^6 \text{ m}^{-1}$ ,  $b = 6 \text{ \AA}$ ,  $T = 300 \text{ K}$ , and  $\Delta p = 1$ ).

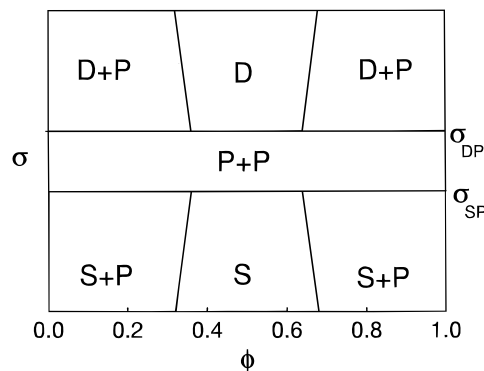


**Figure 4.** Schematic phase diagram for large  $N$  and  $\chi$ , showing the pure-pure coexistence region which appears between the D and S phases.

Notice the following general features. For large  $\sigma$ , we find either a single disordered phase or coexistence of two pure or disordered phases. For lower  $\sigma$ , stripe or stripe-pure coexistence is found. The stripe-pure two-phase region tends to be favored over the hexagonal phase, which is only found at very small  $\sigma$ .

These features can be explained as follows. The disordered phase is preferred at large  $\sigma$  because the electrostatic interaction is strongest when the polymer headgroups are tightly packed, and the extra electrostatic energy of the stripe phase outweighs the saving in mixing energy. Increasing the molecular weight, however, disfavors the disordered phase, because the energy of mixing becomes greater.

For small  $\sigma$  (less than  $\sigma_c$ ) the phases must be either striped, hexagonal, or pure. The extra electrostatic energy in the hexagonal phase is proportional to  $(\phi h_b(\phi))^{1/2}$ , Figure 1. This is convex in  $\phi$ , and therefore unstable against phase separation. The result is regions of composition  $\phi = 0.5$  and  $\phi = 0$  or  $1$ , which are striped and pure respectively. This is why the hexagonal phase appears only at very small  $\sigma$ , where the electrostatic interaction is weak.

In the region  $\sigma > \sigma_c$ , only the disordered phase need be considered. A single phase is stable if  $\partial^2 F_d / \partial \phi^2$  is positive for all  $\phi$ . Now, taking  $p_A = -p_B = 1$

$$\frac{1}{\sigma T} \frac{\partial^2 F_d}{\partial \phi^2} = -2N\chi + \left( \frac{1}{\phi} + \frac{1}{1-\phi} + \frac{4}{\phi-1/2} \right) \quad (37)$$

The quantity in brackets is greater than or equal to 19.2. We infer that a two-phase region (disordered-disordered) first appears at  $N\chi = 9.6$  and that a single disordered phase is stable for  $N\chi$  smaller than this (for  $\Delta p = 1$ ).

Notice that for large  $N$  and  $\chi$ , the regions of P-D coexistence at the top of the diagram disappear and are replaced by a single P-P region. In fact, the striped and disordered single-phase regions have become disconnected, and the new intermediate region of pure-pure coexistence has appeared, Figure 4. The points  $\sigma_{DP}$  and  $\sigma_{SP}$  where the disordered and stripe phases meet the pure phase are found by equating  $F_d(0)$  with  $F_d(0.5)$  and  $F_s(0.5)$  respectively. For  $\phi = 0.5$  and  $p_A = -p_B = 1$ , the disordered phase has free energy

$$\frac{F_d(0.5)}{\sigma T} = \frac{N\chi}{4} - \ln 2 \quad (38)$$

and the stripe phase has

$$\frac{F_s(0.5)}{\sigma T} = \frac{N\chi}{4} \left( \frac{\sigma}{\sigma_c} \right)^{1/2} \quad (39)$$

while the pure phase ( $\phi = 0$  or 1) has energy

$$\frac{F_d(0)}{\sigma T} = 2 \left( \ln \frac{\sigma}{2\sigma_0} - 1 \right) \quad (40)$$

Setting  $F_d(0)$  equal to  $F_d(0.5)$  gives

$$\sigma_{DP}/\sigma_0 = 2^{1/2} \exp(1 + N\chi/8) \quad (41)$$

and to  $F_s(0.5)$  gives

$$\frac{N\chi}{8} \left( \frac{\sigma_{SP}}{\sigma_c} \right)^{1/2} = -1 + \ln(\sigma_{SP}/2\sigma_0) \quad (42)$$

The value of  $N$  for which the disconnection occurs may be obtained by setting  $\sigma_c = \sigma_{DP}$  (or  $\sigma_{SP}$ ). The resulting equation can be solved numerically, with  $\ln \chi$  as a perturbation parameter. The result, for  $\kappa b = 6 \times 10^{-4}$  and  $\Delta p = 1$ , is

$$N\chi = 79.4 + 4.45 \ln \chi \quad (43)$$

For  $\chi = 0.1$ ,  $N_c = 692$ . An approximate result for  $\sigma_{SP}$  may be obtained by replacing the weak logarithmic variation on the right-hand side of eq 42 with a constant, and matching at  $N = N_c$ . This gives

$$\frac{\sigma_{SP}}{\sigma_c} \approx \left( \frac{N_c}{N} \right)^2 \quad (44)$$

The most important question to be resolved is whether a modulated phase can be observed in a polymer monolayer at all. The disorder–stripe disconnection phenomenon described above occurs only for fairly large values of  $N$ , so we can assume that stripes will appear as long as  $\sigma < \sigma_c$ . Now,  $\sigma_c = (5.67 \times 10^{-4} \text{ Å}^{-2}) N\chi^{3/2} \Delta p^2$  for  $b = 6 \text{ Å}$ , so using the estimate of  $\sigma_{\min}$  from section 3

$$\sigma_c/\sigma_{\min} = 0.018 N^{4/3} \chi^{3/2} / \Delta p^2 \quad (45)$$

For  $\sigma_c$  to be greater than  $\sigma_{\min}$ , we require

$$N > 20(\Delta p)^{3/2} \chi^{-9/8} \quad (46)$$

For  $\chi = 0.1$  (and  $\Delta p = 1$ ), we must have  $N > 270$ , which is easily attainable. For  $\chi = 0.01$ , then  $N$  must be at least 3600, which might be more difficult.

The hexagonal phase is more difficult to obtain. The numerical phase diagrams show that S–P two-phase coexistence tends to be favored, except at very small values of  $\sigma$ . Now,  $\sigma_{\min}/\sigma_0 \approx 5000$ , so, although a hexagonal phase region is present in several of the diagrams in Figure 3, it is well outside the allowed range of  $\sigma$ . This implies that a hexagonal phase may not be observable at all, except perhaps for a polymer with a small contact angle with water, for which film rupture would not be a problem.

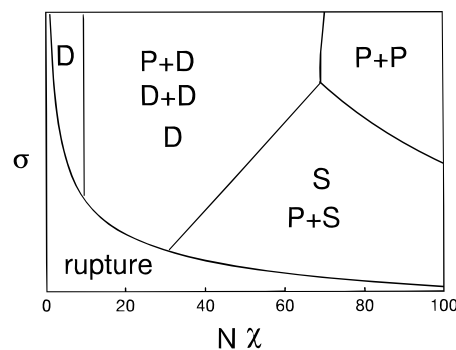


**Figure 5.** Summary phase diagram in the  $N\chi$ – $\sigma$  plane. The diagram shows which phases are to be expected (at different values of the average composition) for given  $N\chi$  and  $\sigma$ . The diagram is calculated for  $\kappa b = 6 \times 10^{-4}$ ,  $\Delta p = 1$ ,  $T = 300 \text{ K}$ , and  $\chi = 0.1$  but will be qualitatively correct for other parameter values; in particular, it depends only weakly on  $\chi$ .

The expected size of the domains is given by eqs 29 and 30. For the stripe, the wavelength is given by

$$\lambda_s^2 = \frac{\pi^3 \epsilon T N b}{e^2 \Delta p^2 \sigma f_s(\phi)} \left( \frac{\chi}{6} \right)^{1/2} \quad (47)$$

and for the hexagonal phase, the radius of the circular domain is

$$\lambda_h^2 = \frac{\epsilon T N b \phi}{4 e^2 \Delta p^2 \sigma f_h(\phi)} \left( \frac{\chi}{6} \right)^{1/2} \quad (48)$$

Since the broadest stripes will be seen for the smallest  $\sigma$ , we take  $\sigma = \sigma_{\min}$ , and with other parameters as  $T = 300 \text{ K}$ ,  $b = 6 \text{ Å}$ ,  $\phi = 0.5$ , and  $\Delta p = 1$ , the stripe wavelength evaluates to  $\lambda_s/\text{Å} = 5.3 N^{2/3} \chi^{1/4}$ . The wavelength is on the order of a few hundred angstroms, if  $N$  is on the order of a few hundred. The effect of salt is beyond the scope of the present theory, but it seems likely that adding enough salt to reduce the Debye length to about  $\lambda_s$  would broaden the stripes. It is possible, however, that this would so weaken the electrostatic interaction that the two polymers would simply phase separate, and the modulated phase would disappear.

The main results are summarized in a semiquantitative fashion in Figure 5, which shows which phases can be obtained (depending on the average composition) at given  $N\chi$  and  $\phi$ . For reasonable parameter values ( $\kappa b = 6 \times 10^{-4}$ ,  $T = 300 \text{ K}$  and  $\Delta p = 1$ ) and  $N\chi < 10$ , there is only uniform mixing of the two components (neither bulk phase separation nor modulated phases). For  $10 < N\chi < 30$ , there are no modulated phases, but the phase diagram contains regions of coexistence of disordered phases. For  $30 < N\chi < 70$ , stripe and pure phases are present at smaller  $\sigma$ ; for larger  $\sigma$ , there is a disordered phase (with  $\phi = 0.5$ ) and pure phases. For  $N\chi > 70$ , there are stripe and pure phases at smaller  $\sigma$  and pure phases only at larger  $\sigma$ . These numerical estimates are obtained from eqs 37, 43, and 46 (note that there is a weak dependence on  $\chi$ ).

## 7. Conclusion

In this paper, a mean-field theory has been developed for the phase behavior of monolayers composed of mixtures of electrically charged amphiphilic polymers. It seems that the most likely behavior is either mixing of the two polymers, or phase separation, or a striped

modulated phase, depending on the degree of polymerization  $N$  and the degree of incompatibility  $\chi$  of the two species. The stripe phase is favored by large  $N$  and  $\chi$  and by a low surface density (i.e., a low surface pressure). The wavelength of the stripe phase is expected to be on the order of 100 Å, longer for larger polymers. Equilibrium states only have been considered here; in practice, it may be difficult to fully equilibrate the system.<sup>8</sup> Furthermore, these conclusions apply only to the case where the water substrate is salt-free and the end-to-end length  $L_0$  is the same for the two species. Obvious extensions of the theory would be the removal of these restrictions.

**Acknowledgment.** This topic of research was suggested by R. Lipowsky, who also made a number of suggestions. The author is also grateful to W. A. Goedel and P. van der Schoot for helpful discussions. This work was funded by the Max-Planck-Gesellschaft.

## References and Notes

- (1) Seul, M.; Andelman, D. *Science* **1995**, *267*, 476.
- (2) Goedel, W. A.; *et al.* *Langmuir* **1994**, *10*, 4209.
- (3) Heger, R.; Goedel, W. A. *Macromolecules* **1996**, *29*, 8912.
- (4) Semenov, A. N. *Sov. Phys. JETP* **1985**, *61*, 733.
- (5) Milner, S. T.; Witten, T. A.; Cates, M. E. *Macromolecules* **1988**, *21*, 2610.
- (6) deGennes, P. G. *Scaling Concepts in Polymer Physics*; Cornell University Press: Ithaca, NY, 1979.
- (7) Adamson, A. W. *Physical Chemistry of Surfaces* (John Wiley and Sons, New York, 1990).
- (8) Möhwald, H. *Ann. Rev. Phys. Chem.* **1990**, *41*, 441.
- (9) Andelman, D.; Brochard, F.; Joanny, J.-F. *J. Chem. Phys.* **1987**, *86*, 3673.
- (10) McConnell, H. M. *Proc. Natl. Acad. Sci. U.S.A.* **1989**, *86*, 3452.
- (11) Goedel, W. A. Private communication.
- (12) Halperin, A. *Europhys. Lett.* **1987**, *4*, 439.
- (13) Cantor, R. S. *J. Chem. Phys.* **1996**, *104*, 8082.
- (14) Hunter, R. *Foundations of Colloid Science* Oxford University Press, Oxford, England, 1986; Vol. 1.
- (15) Chan, D. Y. C.; Mitchell, J. D. *J. Colloid Interface Sci.* **1983**, *95*, 193.
- (16) Mermin, N. D. *Phys. Rev.* **1968**, *176*, 250.
- (17) Kosterlitz, J. M.; Thouless, D. J. *J. Phys. C* **1973**, *6*, 1181.
- (18) Helfand, E.; Tagami, Y. *J. Chem. Phys.* **1972**, *56*, 3592.

MA961448G